SOFT ROBOTICS
Volume 00, Number 00, 2017

DOI: 10.1089/soro.2016.0076

SoRo
Soft Robotics

ORIGINAL ARTICLE

An Implantable Extracardiac Soft Robotic Device for the Failing Heart: Mechanical Coupling and Synchronization

Christopher J. Payne,[1,2,*] Isaac Wamala,[3,*] Colette Abah,[1,2] Thomas Thalhofer,[1,2,4] Mossab Saeed,[3] Daniel Bautista-Salinas,[3] Markus A. Horvath,[1,2,5] Nikolay V. Vasilyev,[3] Ellen T. Roche,[1,2,6] Frank A. Pigula,[3,7,†] and Conor J. Walsh[1,2]

Abstract

Soft robotic devices have significant potential for medical device applications that warrant safe synergistic interaction with humans. This article describes the optimization of an implantable soft robotic system for heart failure whereby soft actuators wrapped around the ventricles are programmed to contract and relax in synchrony with the beating heart. Elastic elements integrated in to the soft actuators provide recoiling function so as to aid refilling during the diastolic phase of the cardiac cycle. Improved synchronization with the biological system is achieved by incorporating the native ventricular pressure in to the control system to trigger assistance and synchronize the device with the heart. A three-state electro-pneumatic valve configuration allows the actuators to contract at different rates to vary contraction patterns. An *in vivo* study was performed to test three hypotheses relating to mechanical coupling and temporal synchronization of the actuators and heart. First, that adhesion of the actuators to the ventricles improves cardiac output. Second, that there is a contraction–relaxation ratio of the actuators which generates optimal cardiac output. Third, that the rate of actuator contraction is a factor in cardiac output.

Keywords: soft actuation, direct cardiac compression, ventricular assist device, heart failure, robotic implant, artificial muscle

Introduction

Soft-bodied robots made from low modulus materials are an emerging technology gaining interest in the robotics community.[1,2] These devices are inherently compliant and conformable, giving them many advantages over traditional rigid robots. Devices made from compliant materials can be designed for safe operation in environments with humans. For example, researchers have developed soft surgical instrumentation[3–5] and compliant robotic catheters that are intrinsically atraumatic.[6,7] A compelling application of this robotic technology is in *assistive* medical devices that warrant synergistic interaction with humans. Examples of this approach include soft exosuits[8,9] and rehabilitative devices.[10,11]

The majority of soft assistive devices have focused on assisting limbs in wearable devices outside of the body. Soft robotic devices have been proposed for cardiac assistance,[12–14] and recently, we proposed a soft robotic implant that can resuscitate and augment cardiac function[15] based on a bioinspired soft actuated material.[13] Such an approach may prove to be a compelling alternative to current therapies for treating heart failure (HF).

[1]John A. Paulson Harvard School of Engineering and Applied Science, Harvard University, Cambridge, Massachusetts.
[2]Wyss Institute for Biologically Inspired Engineering, Harvard University, Cambridge, Massachusetts.
[3]Boston Children's Hospital, Harvard Medical School, Boston, Massachusetts.
[4]Department of Mechanical Engineering, Technical University of Munich, Munich, Germany.
[5]Harvard-MIT Health Sciences and Technology, Massachusetts Institute of Technology, Cambridge, Massachusetts.
[6]Discipline of Biomedical Engineering, College of Engineering and Informatics, National University of Ireland, Galway, Ireland.
[7]Department of Cardiovascular and Thoracic Surgery, University of Louisville School of Medicine, Louisville, Kentucky.
*Joint first authors.
†*Current affiliation*: Jewish Hospital, Rudd Heart and Lung Center, Louisville, Kentucky.

In HF, the heart cannot pump a sufficient blood flow to meet the metabolic demands of the body. HF prevalence in the United States is around 5.7 million people and around half of those diagnosed will die within 5 years of diagnosis.[16] The total financial cost of HF in the United States is estimated at $30.7 billion per year.[16] For patients with advanced HF, transplantation is widely accepted as an effective treatment, but limited donor availability means that many patients will die waiting for a donor heart.

Ventricular assist devices (VADs) provide a means of unloading the heart by supplementing pumping function for patients with advanced HF. The VADs in current clinical practice work by extracting blood from the ventricles or great vessels before pumping the blood back in to the aorta or pulmonary artery so as to assist left or right ventricle function, respectively. VADs can be utilized either as a bridge to transplantation or for permanent implantation in some cases.

The design of VADs has evolved considerably since their very initial use in the 1960s. Nonetheless, clinically approved VADs have largely been based on conventional mechanical pump designs, with the most recent generation utilizing a suspended impeller to provide continuous blood flow.[17–19] Despite clinical uptake, VADs are associated with complications relating to the flow of blood over nonbiologic surfaces which can cause coagulation of the blood and lead to stroke.[20] To mitigate this problem, blood-thinning anticoagulants are commonly prescribed in conjunction with VADs. However, high dosages of anticoagulants can lead to internal bleeding where the VAD has been installed.[20]

Direct cardiac compression devices (DCCs) are an alternative VAD design for augmenting blood flow. These devices assist cardiac function by externally massaging the heart. Since they do not directly contact the blood, the need for blood-thinning agents agents can potentially be avoided altogether along with the associated risks of impeller-based VADs.

A number of DCC designs have previously been investigated.[20–25] Such designs are based on inflatable pneumatic cuffs, which can invert the heart during actuation, and do not provide biomimetic motion to match the native muscle function. This motivated the development of a soft robotic sleeve with integrated soft actuators that are oriented so as to mimic the natural dynamics of the heart.[12,15] The actuators could be programmed to actuate in different modes to stimulate different sides of the heart, provide peristaltic-like sequential contraction, and to provide combinations of contracting and twisting motions.

While DCC devices have demonstrated good ability to compress the heart in the systolic contraction phase of the cardiac cycle, less attention has been given to the diastolic refilling phase. The ability of the ventricles to refill with blood between each cycle is important for sustained cardiac output. Diastole is an active relaxation process;[26] the cardiac muscles store elastic energy during the systolic contraction phase and uncoil in the diastolic phase to cause rapid refilling of the ventricles.[27]

While some DCC devices have been designed to conform to the heart[21] they have not been mechanically coupled in a manner that allows traction forces to be applied during the diastolic cardiac cycle phase to aid ventricle refilling. Vacuum is often used for adhering DCC devices to the heart at the apical region;[22,23] however, the vacuum is not applied directly to the ventricle surfaces to aid diastolic function. Furthermore, previous research has not addressed the effect of mechanical coupling between DCC devices and the heart for either systolic or diastolic function.

Previous DCC devices have aimed to synchronize with the heart using a pacemaker[15] or by detecting the electrocardiogram signal on the heart.[20,21,24,25] The former approach prevents the heart from adjusting to the metabolic requirements of the body and can impede the heart function itself. The electrocardiogram signal triggering method can potentially suffer from temporal variability depending on the condition of the myocardium.[28,29] Finally, irrespective of the triggering methodologies used, previous studies have not considered the optimal synchronization between DCC devices and the heart.

Here we present a modular soft robotic implant for HF that incorporates a series of features to promote diastolic function and temporal synchronization with the native heart. We propose actuators with recoiling ability and a method by which they can be coupled to the heart. This enables enhanced blood refilling during the diastolic phase of the cardiac cycle. Sensing of the real-time hemodynamics using a pressure catheter is used to control and synchronize the device with the natural heart rhythm, forgoing the need for a pacemaker or electrocardiogram triggering methods.

We investigated the intrinsic performance of the soft robotic implant in terms of contraction ability and temporal response. An *in vivo* study was performed to test three hypotheses relating to mechanical coupling and temporal synchronization of the actuators and heart. First, that adhesion of the actuators to the ventricles augments cardiac output. Second, that there is a contraction–relaxation ratio of the soft actuators which generates optimal cardiac output. Third, that the rate of actuator contraction is a factor in determining cardiac output.

Implantable Soft Actuators and Control System

We adopt individual McKibben-based actuators to assist the native heart muscle. McKibben actuators are composed of an inflatable bladder placed within a mesh: when the bladder is pressurized, the mesh contracts linearly and expands radially[30] (Fig. 1).

Our previous work[12,13,15] incorporated multiple actuators in to a sleeve that is wrapped around the heart. In this study, we use individual McKibben actuators that are wrapped around the heart ventricles (shown in Fig. 1). This approach allows the surgeon to systematically position and orient the actuator on the ventricle which allows control over the device placement *in vivo*. The surgeon can choose how many actuators are placed and the size of each can be specified to account for variability between hearts. This also enables an actuator to be placed away from important structures such as the coronary vessels or in regions that might impair function of the valves. The overall size and weight of the implant is also minimized which may allow improved refilling during the diastolic phase.

The McKibben-based actuator design incorporates a pliable wire within the bladder. The ductility of the wire allows the surgeon to individually bend each actuator to fit the shape of the ventricle surface (Fig. 1). Matching the actuator profile to that of the ventricle surface forgoes the need for overtightening which could constrict the ventricle and impede refilling.

Conventional McKibben actuators can generate significant loads in contraction as a result of the bladder pressure.

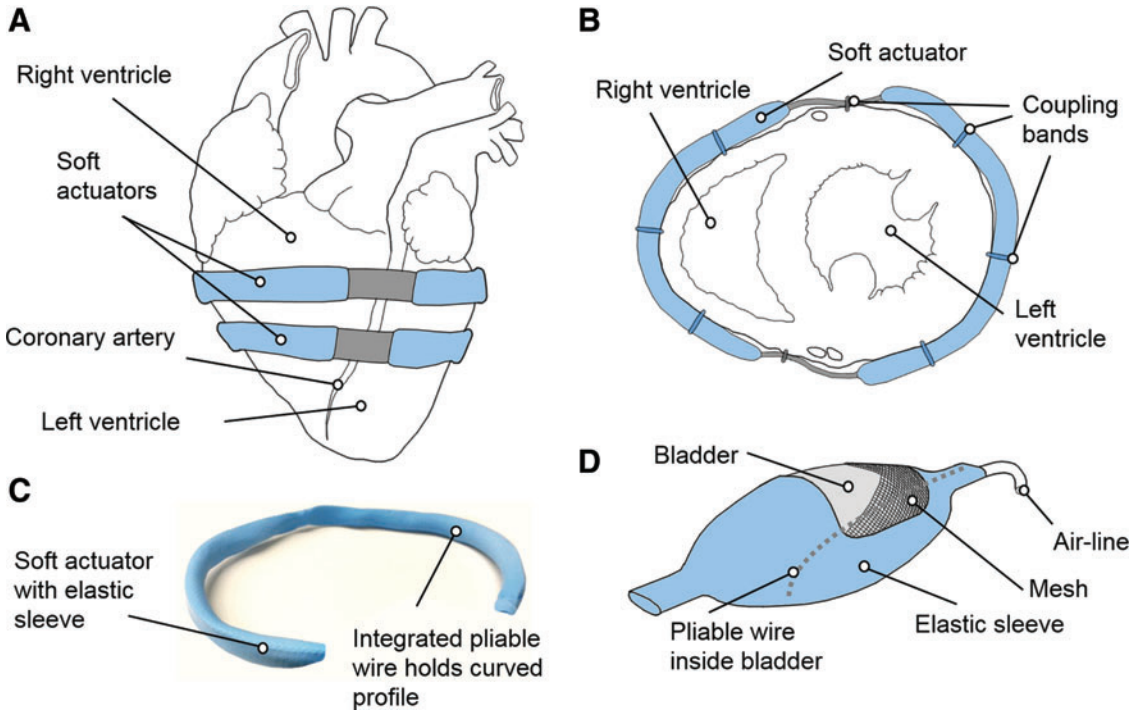

FIG. 1. **(A)** Front view of heart and placement of the actuators. **(B)** Section view of the heart showing the locations of coupling bands that adhere to the ventricle surfaces (three per actuator and two near the septal region). **(C)** Photograph showing a soft actuator configured in to a profile and its shape retained by the integrated ductile wire. **(D)** Shows a section view of the contracted actuator with elastic sleeve and pliable wire within the bladder. Color images available online at www.liebertpub.com/soro

However in relaxation, the force generated is much less and largely determined by elastic energy stored in the actuator mesh structure. In the diastolic relaxation phase of the cardiac cycle, the heart muscles recoil so as to cause rapid refilling.[27] To mimic and enhance this effect in an actuator, we incorporate an elastic sleeve that is placed over the mesh so as to circumferentially stretch during contraction. When depressurized, the elastic energy stored in the stretched sleeve is transferred back to the actuator allowing it to recoil to a fully elongated state (Fig. 2A).

The actuator inner bladders are fabricated from a thermoplastic elastomer (Stretchlon 200; Airtech International).

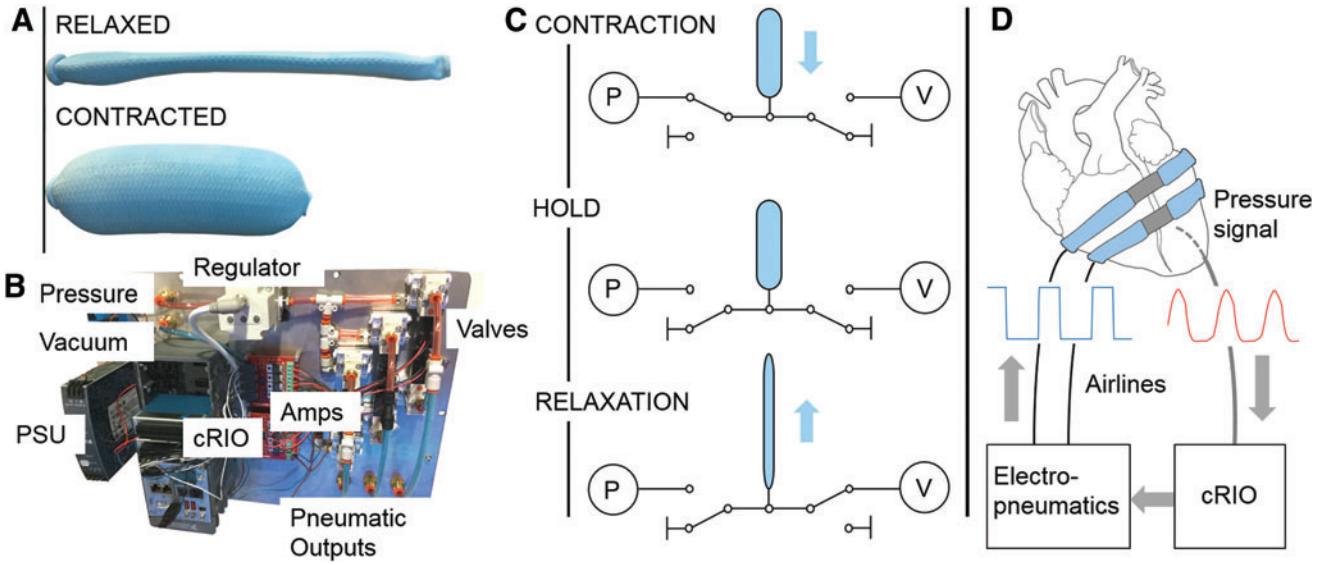

FIG. 2. **(A)** McKibben actuators with elastic sleeve in both relaxed and contracted states. **(B)** Underside view of the control box plate with mounted hardware. **(C)** Schematic of the three-state valve system that allows pressure to be held inside the actuators. **(D)** Pressure triggering control scheme for soft robotic implant. P, pressure; V, vacuum. Color images available online at www.liebertpub.com/soro

This is a 38 μm thick material that can be thermally bonded in to a bladder using a heat press. The inner pliable wire is adhered to the airline and is made to be less than 60% of the length of the bladder so as not to cause rupture of the inner bladder when contracted.

The elastic sleeve is manufactured from dipped rubber of $\sim$250 μm in thickness. In addition to the elastic sleeve, we adhere each actuator to the heart surface using elasticated rubber bands (vessel loops, Medi-Loop®; Medline) of 1.3 mm diameter that are tightly sutured to a point on the ventricle. Like the elastic sleeve, the elastic coupling bands can also stretch in systole and transmit stored elastic energy back to the heart in diastole.

Triggering and control system

Achieving temporal synchronization between the actuators and ventricle is essential for ensuring good augmentation of cardiac function. We previously controlled this synchronization in an open loop manner, using a pacemaker to contract the heart and provide an input to our control system.[15] A drawback to this approach is that use of the pacemaker can interfere with the native cardiac synchronization and further diminish contractility in the heart.

In this study, we propose a pressure catheter (Scisense; Transonics, Inc.) inside the left ventricle (LV) to sense the systolic phase of the cardiac cycle, allowing the control system to trigger the actuators in sync with the native physiology. The signal from the pressure catheter is acquired by the control system and a thresholding function is used to trigger the actuators when the pressure rises 2 mmHg above the diastolic baseline pressure.

A control box incorporates the electro-pneumatic hardware required to contract and relax the actuators (Fig. 2B). We use a field programmable gate array integrated with a real-time controller (cRIO 9030; National Instruments) for the computational control of the actuators. Field effect transistor-based amplifiers are used to actuate a series or pneumatic valves (NVKF333-5G-01T; SMC Corporation) according to the controller output. The valves are arranged so that the actuators can be subject to three conditions; inflation; pressure hold; and deflation (Fig. 2C).

This three-state system allows for modulation of the contraction response time by altering the input flow rate and valve opening time. A regulator is used to maintain the output pressure at a preset, which is also controlled by the real-time controller. A host PC can be connected to the control box, so that variables (such as set-point pressure and actuation period) can be issued to the real-time controller. Similarly, data are passed back to the host to provide a graphical user interface of the real-time data stream during experimentation.

Device Characterization

Pressure–contraction relationship

McKibben actuators have been extensively characterized with respect to contraction ratio and force.[12,13,15,31] We performed characterization tests to study the effect of the elastic sleeve in terms of the pressure–contraction relationship. McKibben actuators were coupled to a calibrated linear potentiometer that measures contraction distance (Fig. 3A). A pressure sensor (BSP000W; Balluff) was connected between the pneumatic output from the control box and the actuator so as to measure the instantaneous pressure in the actuator itself. A data logging system (PowerLab; ADInstruments) running at 1 kHz was used to acquire the data. The control system was commanded to apply a range of pressures from 0 to 45 psi in 1 psi increments. To illustrate the effect of the elastic sleeve on contraction profile, we characterized 100 mm long actuators with and without the elastic sleeve. These pressure–contraction relationships are presented in Figure 3B.

It can be observed that the pressure–contraction relationship of the sleeveless actuator follows a nonlinear profile that is comparable to other McKibben actuators reported in the

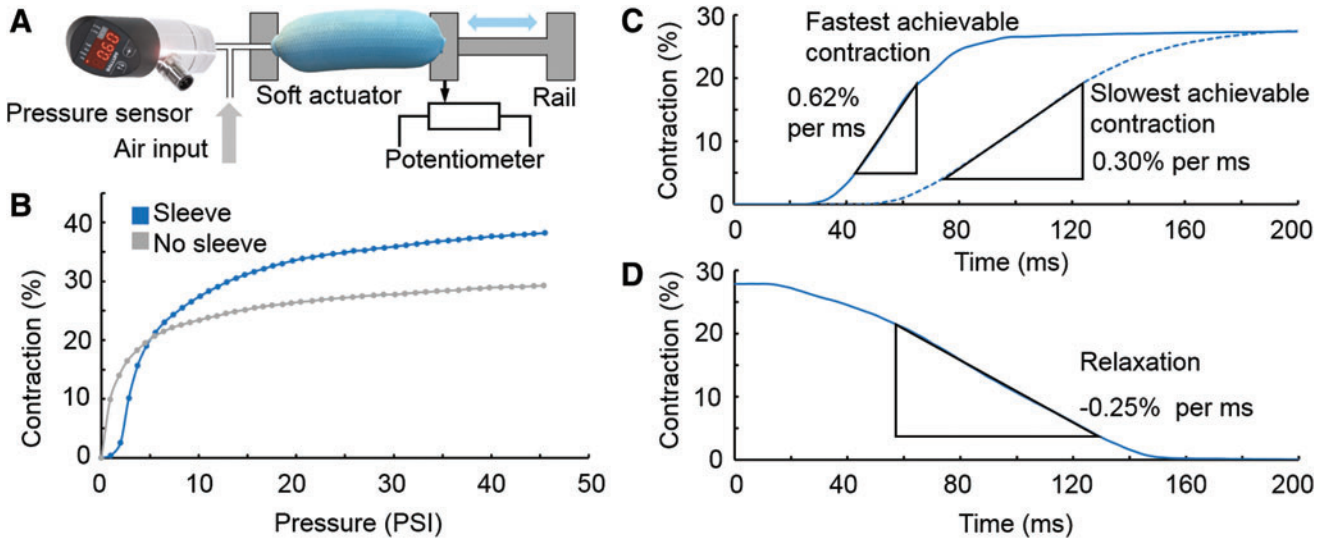

FIG. 3. **(A)** Shows the experimental setup for the characterization tests. **(B)** Shows the pressure–contraction relationships for 100 mm long McKibben actuators with the elastic sleeve (*blue*) and without (*gray*). **(C)** Plot showing the fastest and slowest contraction response allowed by the control system (valves change state at 0 s). **(D)** Plot showing the actuator relaxation (valves change state at 0 s). Color images available online at www.liebertpub.com/soro

literature.[13,31] The total contraction of the sleeveless design at 45 psi was 29%. Greater contraction was observed with the sleeved actuator (38% at 45 psi) since it is contracted from a fully elongated state.

For the sleeved actuator, Figure 3 highlights that a pressure threshold is required before significant contraction is observed in the actuator. This is due to the nonlinear rubber modulus and the nonlinear loading condition of the rubber. A greater pressure is required to achieve the same contraction as the sleeveless actuator due to the additional energy that is required to stretch the sleeve during pressurization. The improved contraction function is significant for the proposed cardiac application as it allows the ventricle wall to fully relax in the diastolic phase and contract by a greater distance in systole.

Contraction rate

We performed an experiment to quantify the slowest and fastest response times to achieve full contraction using a sleeved 100 mm actuator ($n=6$ runs). The actuator was coupled to the calibrated linear potentiometer so that the contraction length could be measured over time (setup shown in Fig. 3). A second signal which indicated when the valve system changed state was acquired simultaneously. To determine the slowest time to full contraction, the regulator was configured to a pressure set point of 10 psi and the valve was opened to enable pressurization. To determine the maximum contraction time, we use the three-state valve system to control the volume of air that is injected in to the actuator.

The regulator was configured to provide a maximum flow rate (pressure set point of 45 psi), and the valve was opened for a set time period of 45 ms (empirically determined) before being shut off to achieve a pressurization of 10 psi. Finally, when the actuator was pressurized at 10 psi, a vacuum of −11.6 psi was applied to the actuator to quantify the relaxation time. The results are shown in Figure 3C, D.

The contraction-time profiles demonstrate that the contraction response time can be varied significantly through different control methodologies. There is a latent contraction time period in both cases due to the valve response time and the minimum pressure threshold required to initiate contraction. In the linear region of the fastest actuator contraction profile, a rate of 0.62% per ms (SD ±0.040% per ms) was attained, in the slowest profile the peak rate was 0.30% per ms (SD ±0.003% per ms). The overall response times to achieve full contraction for the fastest and slowest profile were 120.3 ms (SD ±2.1 ms) and 179.5 ms (SD ±2.4 ms), respectively. In relaxation, the actuator returns to its fully elongated state in 156.0 ms (SD ±1.4 ms) and achieved a peak relaxation rate of 0.25% per ms (SD ±0.001% per ms).

In Vivo Experiments

We carried out an *in vivo* porcine study ($n=1$) to test three hypotheses.

- Hypothesis 1: mechanical coupling between the actuators and ventricle augments cardiac output.
- Hypothesis 2: there is an optimal systolic actuation time period for the device for maximizing cardiac output and diastolic function.
- Hypothesis 3: the rate of actuator contraction is a factor in cardiac output.

In vivo *study setup*

We followed the 1996 guide for the care and use of laboratory animals as recommended by the US National Institute of Health. The study was performed at the Boston Children's Hospital. Ethical approval for the experimental protocol was granted through the Institutional Animal Care and Use Committee. A general anesthetic was induced and mechanical ventilation used to support the swine throughout the surgery. The swine (70 kg) was instrumented with pressure monitoring transducers (SurgiVet; Smiths Medical PM, Inc.) that were located in the left atrium, aorta, pulmonary artery, and right ventricle. A pressure sensor catheter (Scisense; Transonics, Inc.) was placed in the LV, and flow probes (TS420; Transonics, Inc.) were placed on the pulmonary artery and aorta to acquire the blood flow rate through these vessels.

A multichannel data measurement system (PowerLab; AD Instruments) acquired these transducer signals at 1 kHz. The baseline heart rate before implantation was 83 bpm. Two pairs of 100 mm actuators were sutured to the ventricles with elasticated bands (according to the arrangement shown in Fig. 1). To simulate HF we used the drug Esmolol, a short-acting, cardioselective beta blocker which reduces heart rate and contractility. After a steady HF baseline was achieved (heart rate of 72 bpm), we actuated the soft robotic implant at systolic actuation periods of 25%, 30%, 35%, and 40% of the cardiac cycle. The LV pressure signal was used to trigger the robotic implant to contract at the beginning of systole. The heart was allowed to return to the HF baseline levels in between each actuation period. The three elastic coupling bands on each actuator were then removed so that the device was uncoupled from the ventricles.

The robotic implant was then re-actuated at the same timing conditions to allow comparison between the coupled and uncoupled conditions. A linear mixed model statistical analysis was performed to assess significance in comparing multiple variables. The analysis considers repeated measures of aortic flow, pulmonary flow, and end diastolic pressure (15 consecutive cycles). The independent categorical variables were mechanical coupling (bands, no bands) and systolic time period (25%, 30%, 35%, 40%). Data were checked for normality using the Kolmogorov–Smirnov test. Figure 4 shows the implanted device in systole and diastole, with and without the coupling bands. Figure 5 shows the flow rates and LV pressure for a representative cardiac cycle at each condition tested. Figure 6 shows bar plots of the multiple repeated measures for aortic flow, pulmonary flow, and end diastolic pressure under the tested conditions.

Hypothesis 1: Mechanical coupling between actuator and heart improves cardiac output

The experimental results demonstrate that under every timing condition tested, coupling of the actuators to the ventricle significantly improved aortic and pulmonary output ($p<0.001$ for all cases, Fig. 6). Coupling bands augmented aortic flow rate by up to a factor of 2 (Fig. 6A) and the individual aortic ejection volumes per cycle were equivalent to the healthy baseline (mean of 28 mL per ejection).

There are several contributing factors that explain this general trend of improved performance with coupling bands. First, when the device is not coupled to the heart, there is a dead space between the actuators and ventricle (as shown in

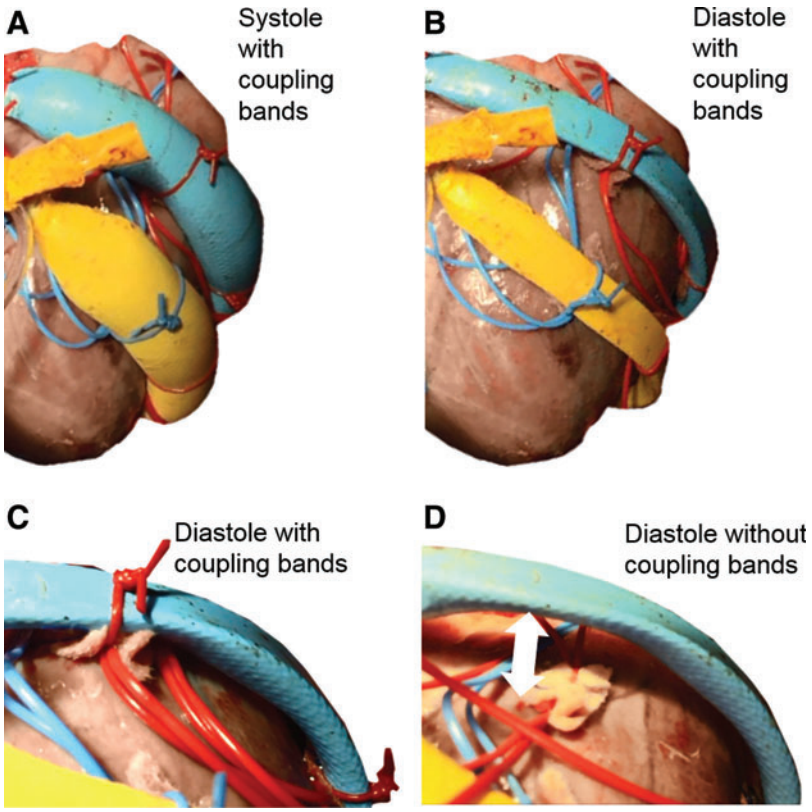

FIG. 4. Images from the *in vivo* study: **(A)** LV and soft robotic device with coupling bands in systole, **(B)** LV and soft actuators with coupling bands in diastole, **(C)** close-up of a soft actuator and coupling band in diastole, and **(D)** close-up of a soft actuator with coupling band released and *arrow* indicating dead zone. Color images available online at www.liebertpub.com/soro

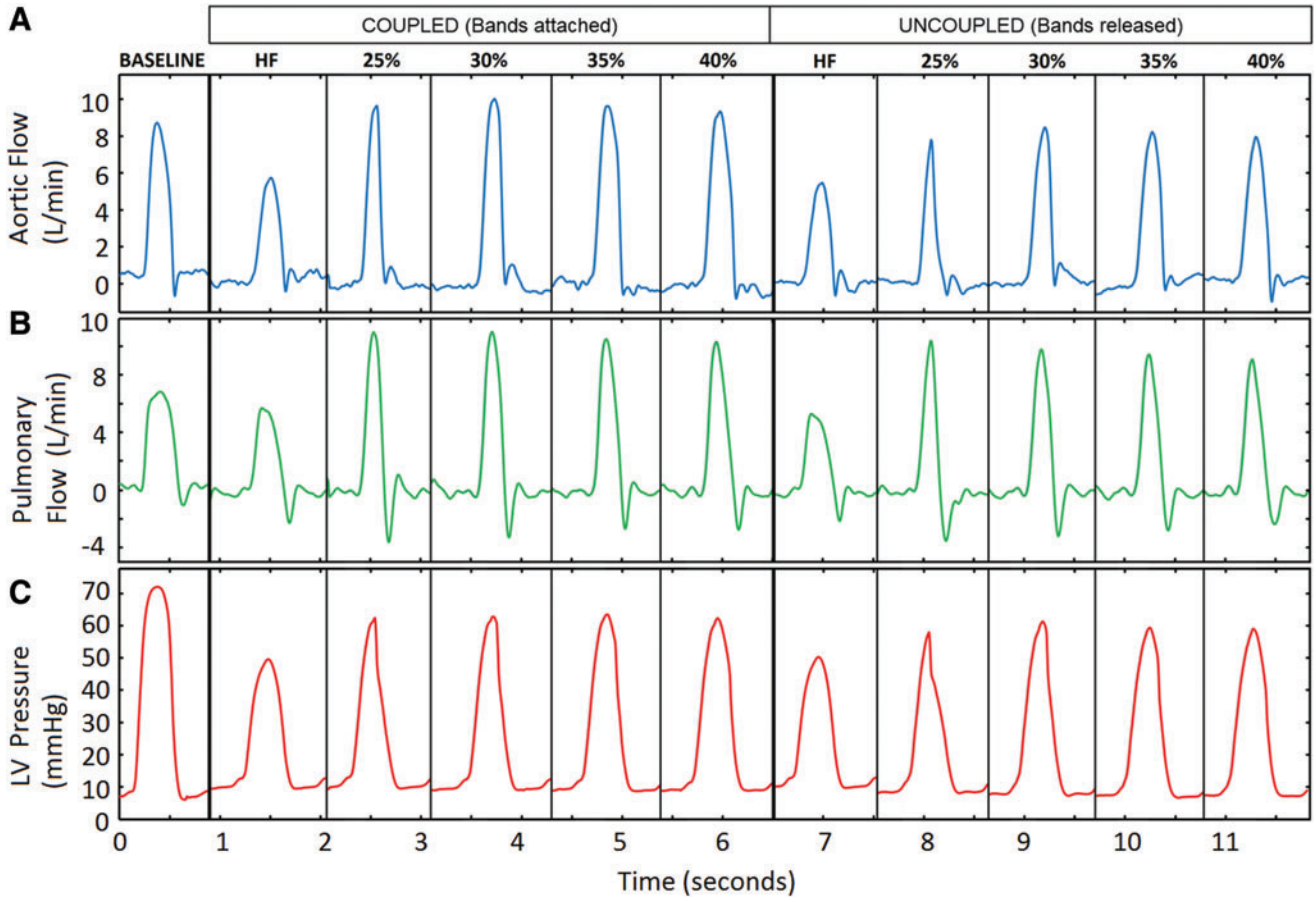

FIG. 5. Plots showing **(A)** aortic flow rate, **(B)** pulmonary flow rate, and **(C)** LV pressure under different systolic actuation timing and mechanical coupling conditions, showing single representative cardiac cycles. Color images available online at www.liebertpub.com/soro

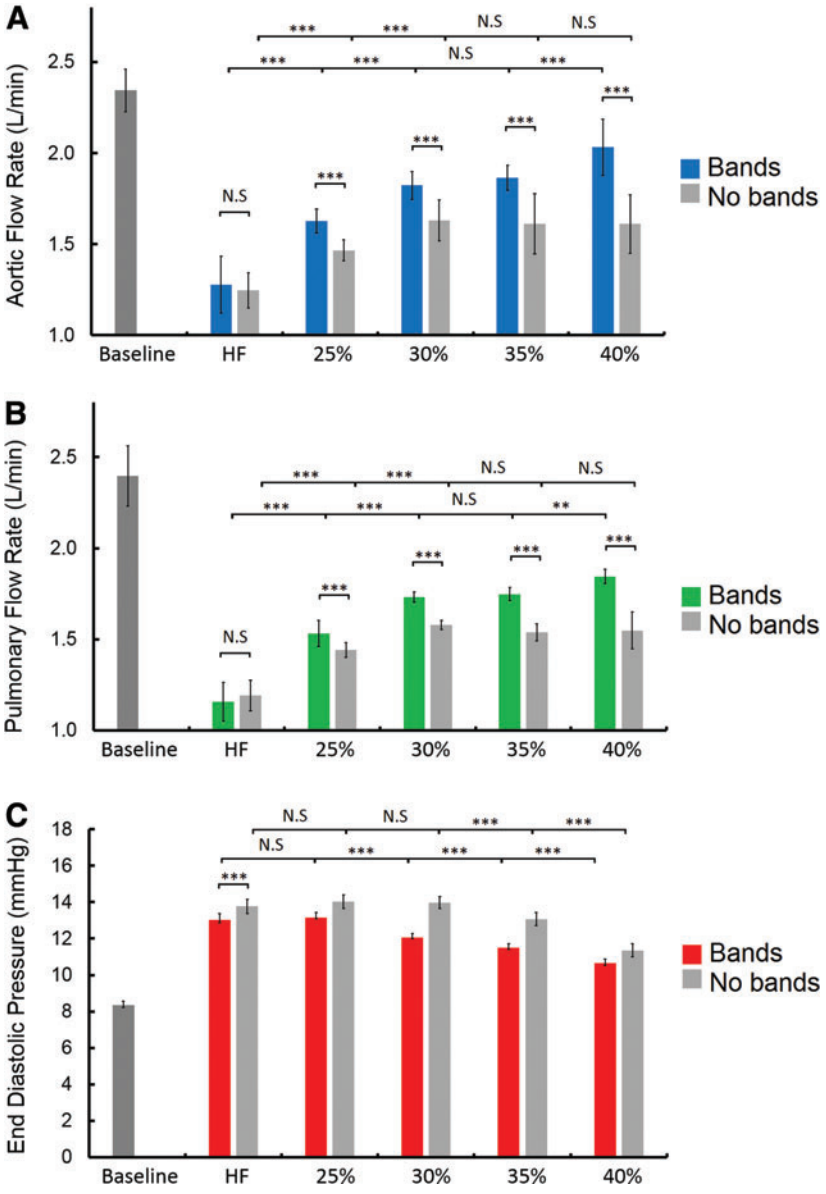

FIG. 6. Bar plots showing **(A)** aortic flow, **(B)** pulmonary flow, and **(C)** end diastolic pressure. ***$p < 0.001$; **$p < 0.01$. Error bars are standard deviations. N.S., not significant. Color images available online at www.liebertpub.com/soro

Fig. 4) which reduces the extent of contraction and recoil that can be transmitted to the heart. Second, in the uncoupled condition, the dead space introduces a time delay before the contracting actuator makes contact with the ventricle in systole, causing an interference with actuator-ventricle synchronization. Third, coupling also constrains the actuators to apply normal forces on to the ventricle and prevents tangential slippage over the ventricle surface.

Hypothesis 2: A longer systolic actuation period improves cardiac function with coupling

The mean aortic and pulmonary flow rates both positively correlate with longer systolic actuation time conditions when the soft robotic device is coupled to the heart. Without coupling, increasing the systolic time period beyond 30% of the cardiac cycle does not yield significant augmentation for either aortic or pulmonary flow rate (Fig. 6). When coupled, a systolic period of 40% was demonstrated to provide the greatest aortic flow rate (2 L/min); this same condition also yielded the greatest pulmonary flow rate (1.8 L/min).

All conditions of device actuation led to a statistically significant increase in cardiac output relative to the HF baseline levels for aortic flow and pulmonary flow ($p < 0.001$ for all cases, Fig. 6). The effect of coupling is most prominent at the 40% actuation period compared to other times. At this longer actuation period, the actuators relax after the heart has entered the diastolic phase and assist with relaxation. At shorter actuation periods, the device recoils before the heart has completed systole and impedes the native contraction, causing lower cardiac output. Furthermore, mechanical coupling may also be more effective at the longer actuation because the time for refilling is reduced.

An encouraging observation was a significant reduction in end diastolic pressure with device operation from HF baseline ($p < 0.001$ for 30–40% systolic period, with coupling bands, Fig. 6C). These results implied improved refilling function of the heart during diastole. A greater drop in end

diastolic pressure at longer systolic actuation times was observed, which is likely due to improved synchronization. At faster heart rates, the effect of the coupling bands may become more prominent when the diastolic phase is shortened and faster recoil is required.

Hypothesis 3: Effect of contraction rate on cardiac output

A second experiment was performed to study the effect of actuator contraction rate. A new HF baseline was established, the heart rate was 73 bpm. The device was actuated using the LV pressure triggering method with a fixed systolic time period of 40% of the cardiac cycle, and the device was coupled to the heart throughout. Using the proposed three-state valve system, we actuated at three different contraction rates: the fastest and slowest contraction response times that our control system could achieve (120 and 180 ms, respectively) and a moderate response time (150 ms), according to the control methodologies outlined in the actuator response time characterization study.

A one-way analysis of variance (ANOVA) with Tukey's post hoc test was used to determine significance ($p < 0.05$) between these conditions. Data were checked for normality using the Kolmogorov–Smirnov test. Analyses were based on 15 consecutive cycles of aortic flow rate, pulmonary flow rate, and systolic pressure. Figure 7 shows example of cardiac cycles under the different conditions. Figure 8 presents bar plots that show average flow rates for aortic and pulmonary flow under the different contraction rate conditions.

The slowest actuator contraction rate significantly augmented aortic and pulmonary flow compared to the faster rates of contraction ($p < 0.001$ in all cases, Fig. 8). The systolic LV pressure was also significantly increased at the slowest contraction rate compared to the faster rates ($p < 0.001$ in all cases Fig. 8C). It is possible that the rapid contraction disrupts the isovolumetric contraction phase of the cardiac cycle, causing premature ventricular ejection and a loss of pressure for the remainder of the cycle. In Figure 7, double peaks can be observed in the LV pressure and aortic flow profiles which is caused by the actuator contracting

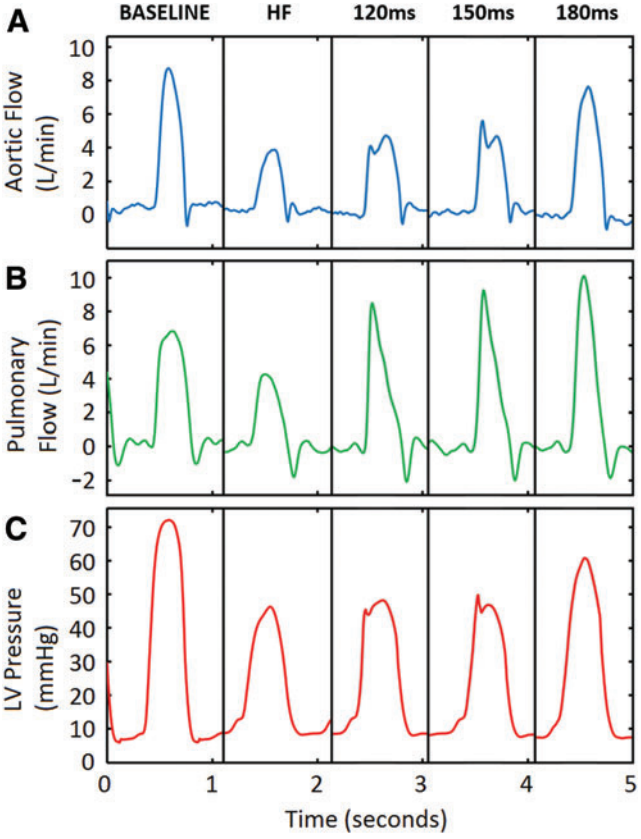

FIG. 7. Plots showing **(A)** aortic flow rate, **(B)** pulmonary flow rate, and **(C)** LV pressure under different contraction rate conditions (unloaded response times of 120, 150, and 180 ms), showing single representative cardiac cycles. Color images available online at www.liebertpub.com/soro

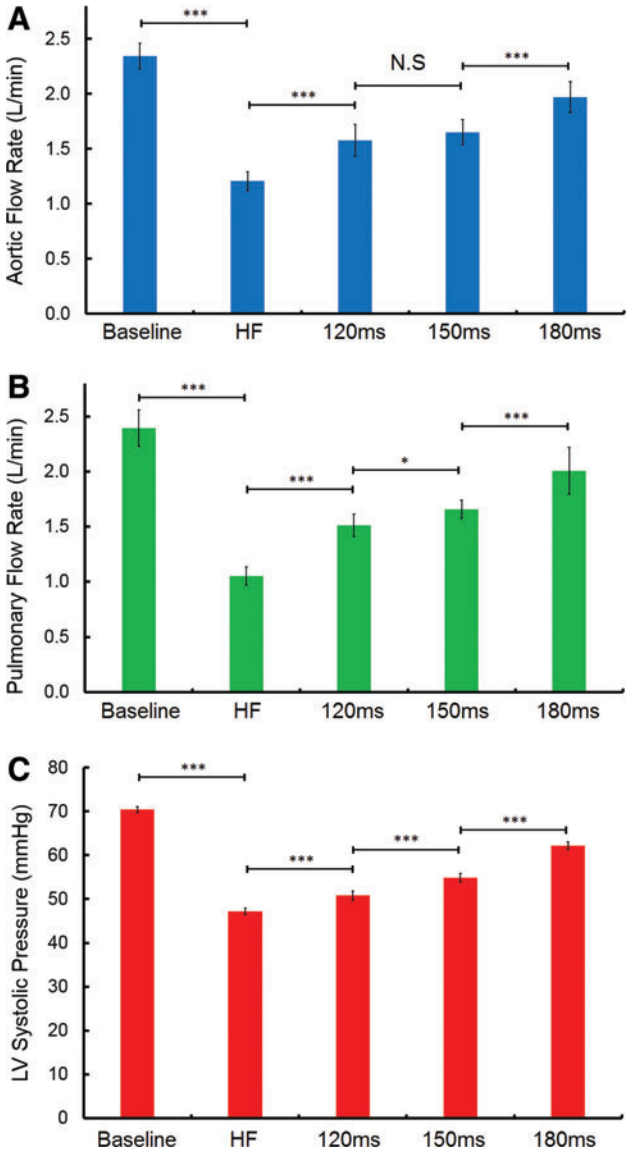

FIG. 8. Bar plots showing **(A)** aortic flow, **(B)** pulmonary flow, and **(C)** systolic pressure for the different rates of soft actuator contraction (unloaded response times of 120, 150, and 180 ms). ***$p < 0.001$; *$p < 0.05$; N.S., not significant. Error bars are standard deviations. Color images available online at www.liebertpub.com/soro

faster than the heart muscles. These experiments demonstrate that systolic synchronization between actuator contraction rate and native heart contraction rate is an important design criterion for DCC devices.

Conclusions and Future Work

This work has demonstrated a series of advancements in the application of soft robotics to cardiac assisting devices. We proposed a soft robotic device design with: (1) recoiling ability to refill the heart; (2) a method of device adhesion to the ventricles to enable diastolic assistance; (3) a control system based on real-time hemodynamics for synchronization with the native heart; (4) configurable actuators that can be formed *in situ* to fit the ventricle; and (5) a control system that allows different rates of actuator contraction to optimize system performance.

The *in vivo* results highlight some important trends. Mechanical coupling between the actuators and native heart showed a consistently significant augmentation on cardiac output. The importance of accurate temporal synchronization between external cardiac compression devices and the native heart was also evident in these studies. Actuation of the device when coupled to the heart at a longer systolic time produced greater cardiac output and a significant reduction in end diastolic pressure. The rate of actuator contraction in systole also significantly affected the cardiac output.

The results presented in this work open many possibilities for further optimization of soft robotic DCC devices. Further work is needed to determine the optimum contraction rate profile for soft actuator-based DCC devices. Additional *in vivo* studies are needed to fully quantify the influence of the effect of the elastic sleeve on actuator recoiling function, as well as the coupling stiffness between actuator and heart. The actuators themselves can be mechanically tuned to have an inherent temporal response and electro-pneumatic control strategies will enable arbitrary actuator contraction characteristics. Emerging soft robotic sensing and control technologies[1] will also enable improved designs for cardiac applications. New actuator designs with improved reliability will be another significant consideration for future soft robotic implants.[32]

For practical deployment, it will also be important to characterize the contraction and relaxation response with clinically relevant working fluids such as helium. While further efforts are required to miniaturize the control system so that it can be worn around the waist of the patient, there is precedent for pneumatic-powered cardiac devices such as the FDA-approved SynCardia™ total artificial heart.[33] Despite this, alternative actuation modalities may enable smaller, more efficient control units to achieve similar cardiac augmentation for future extracardiac VAD designs. Future work will explore different actuation strategies for the left and right ventricles to independently optimize performance for both sides of the heart. Our previous DCC device utilized both circumferential and helically oriented actuators to achieve ejection[15]; mechanical coupling of these additional actuators in such a design may also further augment diastolic refilling.

Robot-tissue adhesion is another remaining challenge for soft robotic implants as less invasive alternatives to suturing will reduce trauma to the tissue surface and provide a more intimate coupling to the biological tissue. For example, the use of tough hydrogels[15,34,35] may facilitate coupling and friction reduction between actuator and ventricle. Mesh-like devices such as the CorCap (Acorn Cardiovascular, Inc.)[36] may also prove effective for generating a biological interface between the soft actuators and heart surface.

Acknowledgments

The authors thank Zurab Machaidze of the Department of Cardiac Surgery, Boston Children's Hospital, and Naomi Crilley, Elizabeth Pollock, Dana Bolgen, and Arthur Nedder of the Animal Research Children's Hospital staff at Boston Children's Hospital for their help with this project. We also thank David Zurakowski of the Department of Anesthesia, Boston Children's Hospital for his assistance. This project was funded by the Translational Research Program grant from Boston Children's Hospital and a Director's Challenge Cross-Platform grant from the Wyss Institute for Biologically Inspired Engineering, Harvard School of Engineering and Applied Sciences.

Author Disclosure Statement

No competing financial interests exist.

References

1. Rus D, Tolley MT. Design, fabrication and control of soft robots. Nature 2015;521:467–475.
2. Holland DP, Park EJ, Polygerinos P, Bennett GJ, Walsh CJ. The soft robotics toolkit: shared resources for research and design. Soft Robot 2014;1:224–230.
3. Cianchetti M, Ranzani T, Gerboni G, Nanayakkara T, Althoefer K, Dasgupta P, *et al.* Soft robotics technologies to address shortcomings in today's minimally invasive surgery: the STIFF-FLOP approach. Soft Robot 2014;1:122–131.
4. Shiva A, Stilli A, Noh Y, Faragasso A, De Falco I, Gerboni G, *et al.* Tendon-based stiffening for a pneumatically actuated soft manipulator. IEEE Robot Autom Lett 2016;1:632–637.
5. Stilli A, Wurdemann HA, Althoefer K. Shrinkable, stiffness-controllable soft manipulator based on a bio-inspired antagonistic actuation principle. 2014 IEEE/RSJ International Conference on Intelligent Robots and Systems 2014;2476–2481.
6. Ikuta K, Ichikawa H, Suzuki K, Yajima D. Multi-degree of freedom hydraulic pressure driven safety active catheter. Proceedings of the 2006 IEEE International Conference on Robotics and Automation, Orlando, FL, 2006; pp. 4161–4166.
7. Rafii-Tari H, Payne CJ, Yang G-Z. Current and emerging robot-assisted endovascular catheterization technologies: a review. Ann Biomed Eng 2014;42:697–715.
8. Bae J, De Rossi SMM, O'Donnell K, Hendron KL, Awad LN, Dos Santos TRT, *et al.* A soft exosuit for patients with stroke: feasibility study with a mobile off-board actuation unit. IEEE International Conference on Rehabilitation Robotics (ICORR), 2015; pp. 131–138.
9. Asbeck AT, De Rossi SM, Holt KG, Walsh CJ. A biologically inspired soft exosuit for walking assistance. Int J Robot Res 2015;34:744–762.
10. Polygerinos P, Galloway KC, Sanan S, Herman M, Walsh CJ. EMG controlled soft robotic glove for assistance during

activities of daily living. IEEE International Conference on Rehabilitation Robotics (ICORR), 2015; pp. 55–60.
11. Cezar CA, Roche ET, Vandenburgh HH, Duda GN, Walsh CJ, Mooney DJ. Biologic-free mechanically induced muscle regeneration. Proc Natl Acad Sci 2016;113:1534–1539.
12. Obiajulu SC, Roche ET, Pigula FA, Walsh CJ. Soft pneumatic artificial muscles with low threshold pressures for a cardiac compression device. ASME 2013 International Design Engineering Technical Conferences and Computers and Information in Engineering Conference, Portland, OR. American Society of Mechanical Engineers, Vol. 6A: 37th Mechanisms and Robotics Conference, pp. V06AT07A009.
13. Roche ET, Wohlfarth R, Overvelde JTB, Vasilyev NV, Pigula FA, Mooney DJ, *et al.* A bioinspired soft actuated material. Adv Mater 2014;26:1200–1206.
14. Mac Murray BC, An X, Robinson SS, van Meerbeek IM, O'Brien KW, Zhao H, *et al.* Poroelastic foams for simple fabrication of complex soft robots. Adv Mater 2015;27:6334–6340.
15. Roche ET, Horvath MA, Wamala I, Alazmani A, Song S-E, Whyte W, *et al.* Soft robotic sleeve supports heart function. Sci Transl Med 2017;9:eaaf3925.
16. Mozaffarian D, Benjamin E, Go A, Arnett D, Blaha M, Cushman M, *et al.* Heart disease and stroke statistics-2016 update: a report from the American Heart Association. Circulation 2016;133:e38–e360.
17. Givertz MM. Ventricular assist devices: important information for patients and families. Circulation 2011;124:305–312.
18. Rodriguez LE, Suarez EE, Loebe M, Bruckner BA. Ventricular assist devices (VAD) therapy: new technology, new hope? Methodist DeBakey Cardiovasc J 2013;9:32–37.
19. Rogers JG, Pagani FD, Tatooles AJ, Bhat G, Slaughter MS, Birks EJ, *et al.* Intrapericardial left ventricular assist device for advanced heart failure. N Engl J Med 2017;376:451–460.
20. Oz MC, Artrip JH, Burkhoff D. Direct cardiac compression devices. J Heart Lung Transplant 2002;21:1049–1055.
21. Moreno MR, Biswas S, Harrison LD, Pernelle G, Miller MW, Fossum TW, *et al.* Assessment of minimally invasive device that provides simultaneous adjustable cardiac support and active synchronous assist in an acute heart failure model. J Med Devices 2011;5:041008.
22. Anstadt GL. Heart massage apparatus. United States patent US5119804. 1992.
23. Lowe JE, Hughes GC, Biswas SS. Non–Blood-Contacting Biventricular Support: Direct Mechanical Ventricular Actuation. Oper Tech Thorac Cardiovasc Surg 1999;4:345–351.
24. Kavarana MN, Loree HM 2nd, Stewart RB, Milbocker MT, Hannan RL, Pantalos GM, *et al.* Pediatric mechanical support with an external cardiac compression device. J Cardiovasc Dis Diagns 2013;1:1000105.
25. Artrip JH, Yi G-H, Levin HR, Burkhoff D, Wang J. Physiological and hemodynamic evaluation of nonuniform direct cardiac compression. Circulation1999;100:II236–II243.
26. Pouleur H. Diastolic dysfunction and myocardial energetics. Eur Heart J 1990;11:30–34.
27. Rademakers FE, Buchalter MB, Rogers WJ, Zerhouni EA, Weisfeldt ML, Weiss JL, *et al.* Dissociation between left ventricular untwisting and filling. Accentuation by catecholamines. Circulation 1992;85:1572–1581.
28. Pueyo E, Sornmo L, Laguna P. QRS slopes for detection and characterization of myocardial ischemia. IEEE Trans Biomed Eng 2008;55:468–477.
29. Kashani A, Barold SS. Significance of QRS complex duration in patients with heart failure. J Am Coll Cardiol 2005;46:2183–2192.
30. Schulte HF. The Characteristics of the McKibben Artificial Muscle. The Application of Extemal Power in Prosthetics and Orthotics. Washington, DC: National Academy of Sciences and National Research Council, 1961.
31. Chou C-PCC-P, Hannaford B. Static and dynamic characteristics of McKibben pneumatic artificial muscles. Proc IEEE Int Conf Robot Autom 1994;281–286.
32. Robertson MA, Sadeghi H, Florez JM, Paik J. Soft Pneumatic Actuator Fascicles for High Force and Reliability. Soft Robot 2017;4:23–32.
33. Slepian MJ, Smith RG, Copeland JG. The SynCardia CardioWest™ total artificial heart. Fundam Clin Cardiol 2006;56:473.
34. Sun J-Y, Zhao X, Illeperuma WR, Chaudhuri O, Oh KH, Mooney DJ, *et al.* Highly stretchable and tough hydrogels. Nature 2012;489:133–136.
35. Darnell MC, Sun J-Y, Mehta M, Johnson C, Arany PR, Suo Z, *et al.* Performance and biocompatibility of extremely tough alginate/polyacrylamide hydrogels. Biomaterials 2013;34:8042–8048.
36. Oz MC, Konertz WF, Kleber FX, Mohr FW, Gummert JF, Ostermeyer J, *et al.* Global surgical experience with the Acorn cardiac support device. J Thorac Cardiovasc Surg 2003;126:983–991.

Address correspondence to:
Frank A. Pigula
Jewish Hospital
Rudd Heart and Lung Center
201 Abraham Flexner Way
Suite 1200
Louisville, KY 40202

E-mail: frank.pigula@ulp.org

Conor J. Walsh
John A. Paulson Harvard School
of Engineering and Applied Science
Harvard University
60 Oxford Street
Cambridge, MA 02138

E-mail: walsh@seas.harvard.edu